

A SOLID-STATE PINGER TUNE MEASUREMENT SYSTEM FOR THE INTENSE PULSED NEUTRON SOURCE (IPNS) RAPID CYCLING SYNCHROTRON (RCS)*

J. C. Dooling[†], L. Donley, M. K. Lien, and C. Y. Yao
Argonne National Laboratory, Argonne, IL 60439, U.S.A.

Abstract

A cw tune measurement system for the IPNS RCS is described. The pinger magnets are energized by a solid-state, transformer-coupled power supply operating at 30 Hz. In its present configuration, the power supply provides a 160-A pulse to a pair of series-connected, single-turn ferrite magnets. The magnet pair separately drive x- and y-plane orbit bumps in the $h=1$ beam. The dipole oscillations generated in the beam are sensed with pairs of split-can, pie electrodes. Raw signals from the H and V electrodes are carried on matched coax cables to 0/180-degree combiners. The output difference signals are recorded with gated spectrum analyzers. Bunch circulation frequency varies from 2.21 MHz at injection to 5.14 MHz at extraction. With a fixed frequency span of 24 MHz, between four and ten bunch harmonics and sidebands (SBs) are present in the difference spectra. Software has been developed to use the multi-harmonic SBs present over the span to improve the accuracy of the tune measurements. The software first identifies and then fits the multiple SBs to determine the tune. Sweeping the beam across the momentum aperture provides a method for measuring the chromaticity.

RCS PINGER DIAGNOSTIC

The IPNS RCS operated for almost 25 years without a dedicated tune diagnostic system [1]. Finally in February 2006, a ferrite pinger magnet set was added [2]. The horizontal and vertical magnets were initially driven by a thyatron-switched transmission line, essentially using 1/4 of the extraction kicker system. Assisted by an AC septum and a combined-function, horizontally defocusing singlet, the kicker provides 24 mrad of deflection, sufficient to extract the 450-MeV proton beam in a single turn. By contrast, the pinger supply need only provide a beam deflection on the order of 0.1-0.5 mrad. Therefore one of the goals of this work is to build a lower power, lower maintenance supply relative to the thyatron-based system. Another goal is to develop a diagnostic that can determine tune and chromaticity values more quickly than the single-shot measurements previously described [2]. In that case, pie-electrode data are recorded on a fast, deep memory oscilloscope. An optimized spectrum is then generated off-line; this process tends to be CPU intensive. In the present study, spectral data are recorded directly using two Agilent E4402B spectrum analyzers (SAs). Signals are first collected in each plane from a pair of split-can pie electrodes [3]. Each signal pair is fed

on matched transmission lines to 0/180-degree combiners producing an A-B output. The x- and y-difference signals are recorded on the gated SAs.

Pinger Power Supply

The power supply combines the properties of SCR-Marx and transformer step-up circuits. The amp-turns of four Marx circuit outputs are summed through a transformer to provide the final output to the pinger magnet load as shown in Figure 1. In addition to the series-connected horizontal and vertical magnet pair, the pinger load includes a 6.2- Ω resistor in parallel with 0.040- μ F of ceramic disk capacitance. The terminating load is shown in Figure 2 prior to installation. To roughly match the terminating load impedance, eight 50- Ω , RG-217 coaxial cables are run in parallel from the pinger supply to the terminating load. Each cable is 7.6-m (25-ft) in length. To provide current protection for the 2N6405 SCRs, a 1.4- Ω series resistor is placed between each Marx stage. Initial testing of the pinger was conducted with two turns on each primary side winding and four turns on the secondary output side. The terminating impedance was connected in series to a single horizontal test magnet.

Several different values of capacitance in parallel with load resistance were tried to see if rise time could be reduced. In Figure 3, pinger output current waveforms are presented for terminating capacitances of 5 and 40 nF. The risetime is seen to improve from 186 to 174 ns as capacitance is raised between these two capacitance values; however, greater oscillations in output voltage and current also occur as the load impedance drops below a matched condition. To reduce hysteresis in the output transformer ferrite, each core is gapped to 0.38 mm (15 mils), lowering the energy per cycle lost in the NiZn core

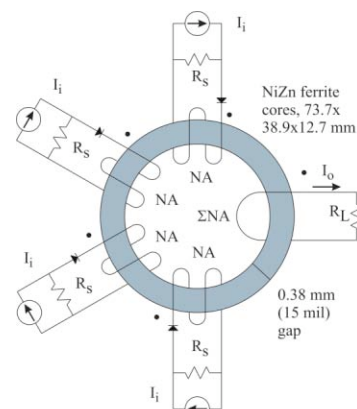


Figure 1: Output transformer schematic.

*Work supported by U.S. DOE, Office of Science, Office of Basic Energy Sciences, under contract number DE-AC02-06CH11357.

[†]jcdooling@anl.gov



Figure 2: Pinger terminating load.

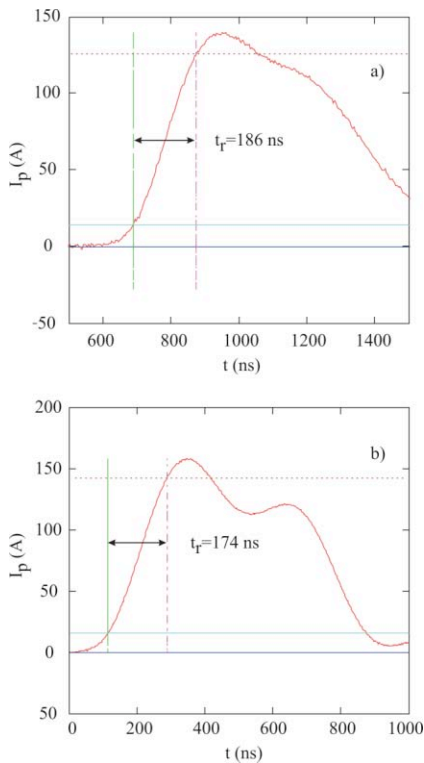


Figure 3: Comparison of 4-turn pinger output current waveforms and risetimes for a) 5 nF and b) 40 nF bypass capacitance.

material. However, this also lowers the inductance of the transformer, which must remain much higher than either the source or load impedances for efficient transformer response. Just prior to installation, the number of toroidal cores in the transformer was increased from five to seven. At the same time, the number of turns on the primary side was reduced from two to one; and the secondary winding was lowered from four to two turns. The pinger was placed into service in this configuration; see Figure 4. Its output was tested into the single test magnet without the terminating load since the load had already been installed in the RCS tunnel. Figure 5 presents the output voltage and current waveforms, the charge voltage on a single Marx capacitor, and the trigger signal at maximum output.

Tune measurements and diagnostics systems

Once the pinger supply was installed, its output current into the actual dual-pinger magnet set and terminating load was monitored with a Pearson Model 6600 current toroid (0.05 V/A, 50 Ω) mounted to the terminating load, as shown in Figure 2. The current waveform into the magnets at the terminating load is presented in Figure 6 for a nominal voltage of 40 percent maximum output. A clear reduction is seen in the FWHM output pulsewidth relative to that shown in Figure 5. Examples of x- and y-difference spectra recorded at 40 percent of maximum output voltage, 10 ms after injection are given in Figure 7.



Figure 4: Final pinger configuration (two turn output).

Tune Algorithm

The algorithm for finding the tune from a recorded spectrum is as follows: For a given time in the acceleration cycle, the fundamental frequency is estimated using a fourth-order polynomial. The algorithm refines this estimate by locating all of the harmonic peaks within a fixed frequency range of 0-24 MHz. The 24-MHz span is represented by 801 points, making the bin width 30 kHz. Video and Resolution Bandwidths (VBW and RBW) are both set to 30 kHz on each SA. The number of harmonics participating in the analysis varies from ten

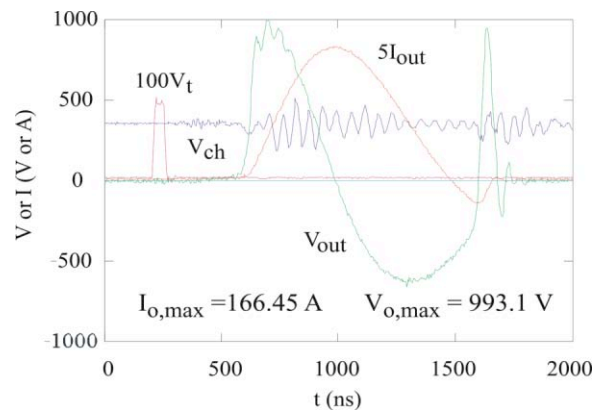


Figure 5: Two-turn output into unterminated magnet load.

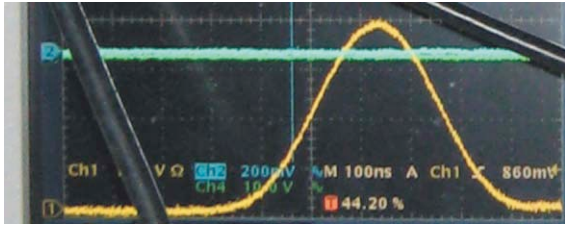


Figure 6: Pinger current waveform (partially obscured), two-turn output, into the terminated load; horiz. scale: 100 ns/div; vert. scale: 1 V/div (50 Ω , term.) = 20 A/div. Output voltage set to 40 percent.

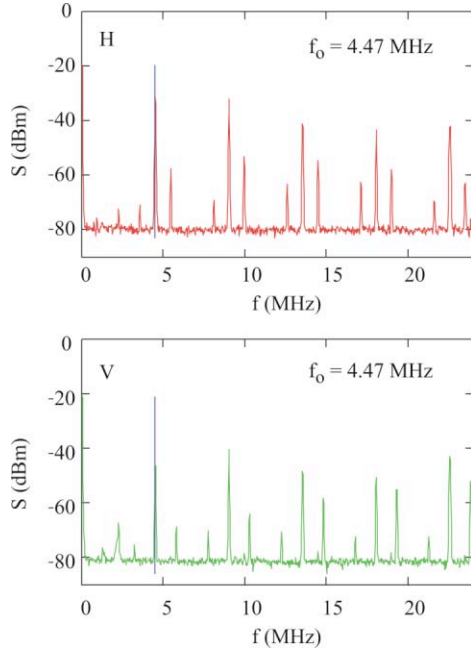


Figure 7: Difference spectra, 10 ms, nominal radial position (central orbit).

near injection ($f_0=2.21$ MHz) to four prior to extraction ($f_0=5.14$ MHz). It is required that all component sidebands of a principal harmonic must be present in the 0-24 MHz span to be included in the tune calculation. The exact location of each peak is determined by calculating the parabola described by the three measured spectral intensities, S_1 , S_2 , and S_3 , about the local maximum. Within the $2\Delta f$ range (60 kHz) including the peak, the spectral amplitude is expressed as,

$$S(f) = a_0 + a_1 f + a_2 f^2, \quad (1)$$

where the coefficients a_0 , a_1 , and a_2 are given as,

$$\begin{aligned} a_0 &= \Delta^{-1} \left[S_1 (f_2 f_3^2 - f_3 f_2^2) + S_2 (f_3 f_1^2 - f_1 f_3^2) + S_3 (f_1 f_2^2 - f_2 f_1^2) \right], \\ a_1 &= \Delta^{-1} \left[S_1 (f_2^2 - f_3^2) + S_2 (f_3^2 - f_1^2) + S_3 (f_1^2 - f_2^2) \right], \\ a_2 &= \Delta^{-1} \left[S_1 (f_3 - f_2) + S_2 (f_1 - f_3) + S_3 (f_2 - f_1) \right], \end{aligned} \quad (2)$$

and Δ is the determinant. The peak intensity occurs when $dS/df=0$ or $f_p = -a_1/2a_2$. The value of the bunch frequency is expressed as the weighted average of all the visible principal harmonics. The locations of the x- and y-sidebands are measured in a fashion similar to the principal harmonics. The tunes are then determined from the total separation of the upper and lower sidebands relative to the bunch frequency. The horizontal fractional bare tune is near 0.18; therefore, the search is made in a range from 0.14-0.22. Fast and slow waves are both present, so the search extends below as well as above the harmonic frequencies. The vertical fractional bare tune is 0.32, and the search in the vertical plane covers a fractional tune range from 0.24-0.33. Space-charge usually lowers the vertical tune. The RCS Tune software display, presented in Figure 8, shows first an acquired vertical spectrum followed by the peak search results.

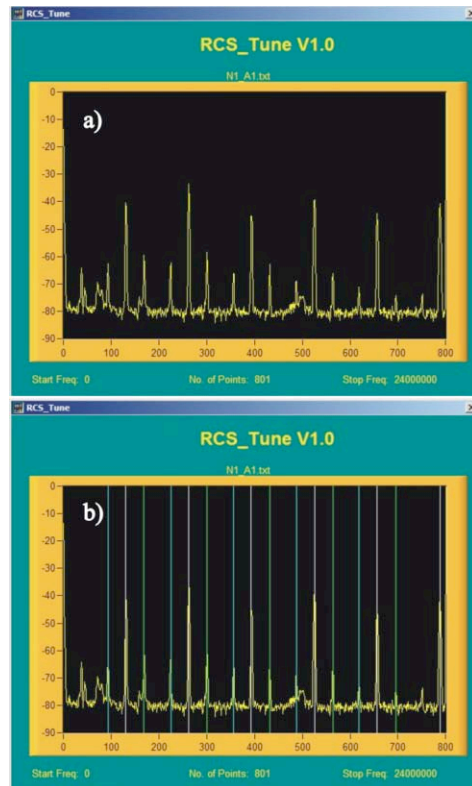


Figure 8: An early version of the RCS Tune software screen a) after reading a difference spectrum and b) after the first localization of peaks. The vertical spectrum is acquired 8 ms after injection.

RESULTS

Tune measurements are made at 1-ms increments during the 14.2-ms acceleration cycle, beginning 1 ms after injection. The period immediately after injection is avoided due to an early, vertical microwave instability. Measurements are made at reduced intensity to minimize the effect of space-charge-dependent tune-shift. Whereas typical injection involves 3.6×10^{12} protons (580 nC), for

tune measurements, approximately 0.5×10^{12} protons are injected (80 nC). At a given time in the cycle, chromaticity is evaluated by stepping the beam across the horizontal aperture using a local change in the frequency.

Examples of tune measurements made with the SS pinger are presented in Figures 9-12; these data were collected 11 and 12 ms after injection. SS Pinger data, obtained in November 2007 are compared with earlier data collected using the thyratron-based diagnostic in May 2007. Central orbit tune and chromaticity data are compared for these two periods in Figures 13 and 14. In general, small variations exist in the central horizontal and vertical tunes. The most significant shift is in the vertical plane where the November data are higher throughout the cycle. Regarding chromaticity, the horizontal data late in the cycle show the November results approaching positive values; in the past, positive x-chromaticity was cited as a

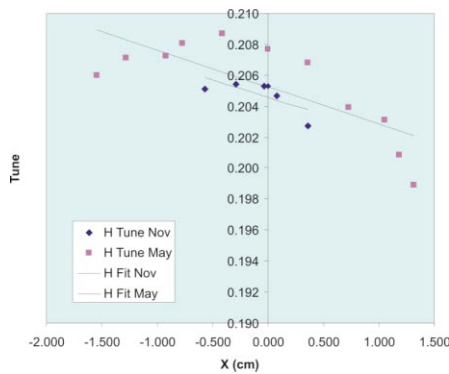


Figure 9: x-tune vs. x-position at 11 ms.

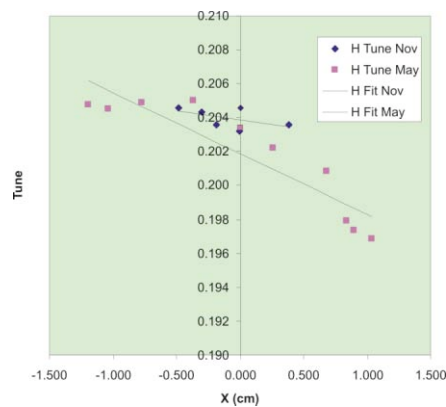


Figure 10: x-tune vs. x-position at 12 ms.

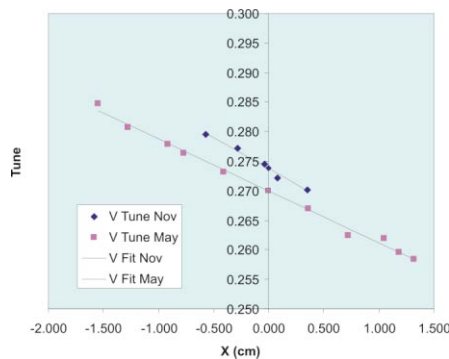


Figure 11: y-tune vs. x-position at 11 ms.

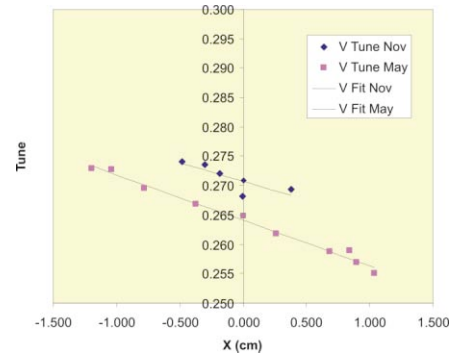


Figure 12: y-tune vs. x-position at 12 ms.

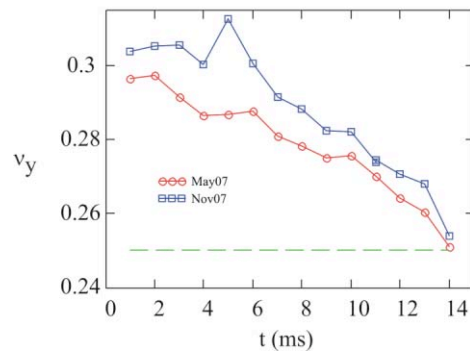
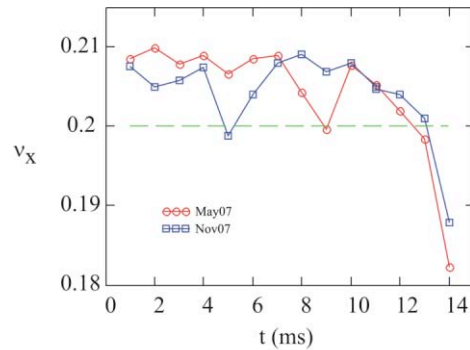


Figure 13: x- and y-tunes throughout the RCS cycle recorded in May and November, 2007.

reason for a head-tail instability that limited the current in the RCS; see the next section for further discussion.

DISCUSSION AND CONCLUSIONS

Chromaticity, the change in focusing relative to a change in momentum or energy, is expressed as

$$\xi(x, s) = \frac{dv}{\left(\frac{dp}{p}\right)} = \frac{v'(x)dx}{\left(\frac{\Delta x}{D(s)}\right)} \approx v'(x)D(s), \tag{3}$$

where $D(s)$ is the local value of dispersion at the pie electrode. When normalized by the tune, chromaticity takes on a value close to -1 for a FODO lattice ring below transition [4]. Pulsed sextupoles are used to control both

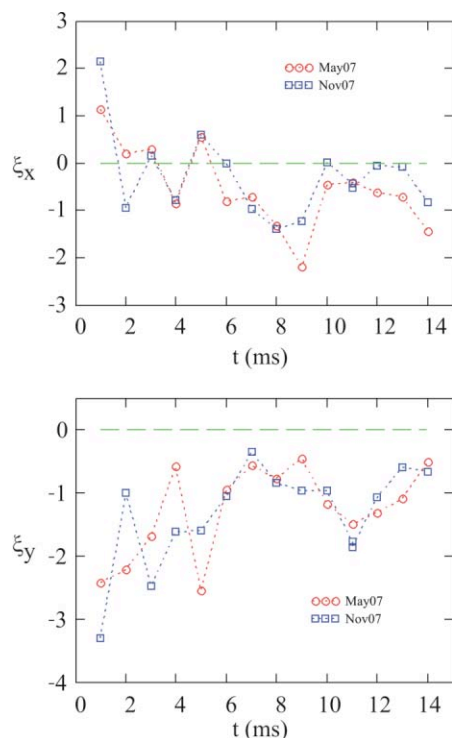


Figure 14: x- and y-chromaticities throughout the RCS cycle recorded in May and November, 2007.

x- and y-chromaticities during acceleration. These magnets were found to be important for stabilizing a horizontal head-tail instability early in the history of the RCS [5,6]. Stabilizing the head-tail allowed the current in the machine to be more than doubled from 4-5 μA to 10-11 μA . At the higher current level a new, vertical instability appeared later in the cycle (>10 ms). The vertical instability is not curable with sextupoles; instead, phase modulation (PM) at twice the synchrotron frequency that leads to quadrupole oscillations and a subsequent high-frequency microwave effect appears to add enough Landau damping to allow operation up to 16 μA . The form of the tune across the horizontal aperture can be represented with a polynomial. The horizontal data shown in Figures 9 and 10 suggest the order of the polynomial should be 2 or higher, indicating the presence of at least octupole terms in the focusing; however, sextupoles can only affect the linear term.

One of the main motivations for the pinger was to try to understand the nature of the instabilities in the RCS that limit its current. It was mentioned that the pulsed sextupole magnets play an important role in stabilizing the beam from destructive head-tail (HT) instabilities. During 2007, the HT reappeared. An example of the change that took place in the horizontal spectrum between 2006 and 2007 is shown in Figure 15. In the former case, at 11 ms in the cycle, only principal beam harmonics were observed; however, in 2007, horizontal sidebands appeared. Average beam current in most cases during this latter period was limited to under 15 μA . Several

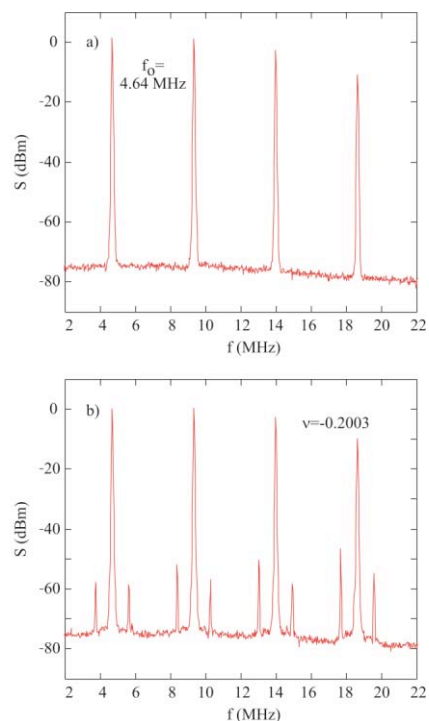


Figure 15: RCS full intensity beam spectra from a single-ended horizontal pie electrode 11 ms after injection a) December 2006 and b) December 2007. The oscillations indicated by the sidebands in b) are self-excited.

attempts were made to adjust sextupoles during 2007, but they proved to be unsuccessful. Having faster tune and chromaticity measurements, as the SS pinger diagnostic was beginning to provide, might have allowed a more coherent effort to mitigate the instability.

In conclusion, the SS pinger system did allow tune and chromaticity results to be obtained more quickly and with comparable accuracy relative to the single-pulse diagnostic.

ACKNOWLEDGEMENTS

On January 1, 2008 the IPNS program was terminated. IPNS set the reliability standard for accelerator-based neutron user facility operations. It was a pleasure to work with the dedicated people that made the IPNS function so smoothly.

REFERENCES

- [1] A. V. Rauchas et al., IEEE Trans. Nuc. Sci. **28**(3), 2331 (1981).
- [2] J. C. Dooling et al., BIW06, AIP-868, 2006, p. 281.
- [3] A. V. Rauchas et al., IEEE Trans. Nuc. Sci. **28**(3), 2338 (1981).
- [4] S. Y. Lee, *Accelerator Physics*, World Scientific, Singapore, 1999, p. 121.
- [5] Y. Cho, A. V. Rauchas, IEEE Trans. Nuc. Sci. **28**(3), 2585 (1981).
- [6] C. Potts et al., IEEE Trans. Nuc. Sci. **28**(3), 3020 (1981).